Helmholtz-Zentrum Dresden-Rossendorf (HZDR)

HELMHOLTZ ZENTRUM
DRESDEN ROSSENDORF

Solution species and crystal structure of Zr(IV) acetate

Hennig, C.; Weiss, S.; Kraus, W.; Kretzschmar, J.; Scheinost, A.;

Originally published:

February 2017

Inorganic Chemistry 56(2017), 2473-2480

DOI: https://doi.org/10.1021/acs.inorgchem.6b01624

Perma-Link to Publication Repository of HZDR:

https://www.hzdr.de/publications/Publ-23922

Release of the secondary publication
on the basis of the German Copyright Law § 38 Section 4.

Solution species and crystal structure of Zr(IV) acetate

Christoph Hennig[1,2], Stephan Weiss[1], Werner Kraus[3], Jerome Kretzschmar[1], Andreas C. Scheinost[1,2]

[1]Helmholtz-Zentrum Dresden-Rossendorf, Institute of Resource Ecology, Bautzner Landstrasse 400, 01328 Dresden, Germany

[2]The Rossendorf Beamline at ESRF, BP 220, 38043 Grenoble, France

[3]BAM Federal Institute for Materials Research and Testing, Richard-Willstätter-Str. 11, D-12489 Berlin, Germany

Abstract

The complex formation and the coordination of zirconium with acetic acid were investigated with Zr K-edge EXAFS spectroscopy and single crystal diffraction. Zr K edge EXAFS spectra show that a stepwise increase of acetic acid in aqueous solution with 0.1 M Zr(IV) leads to a structural rearrangement from initial tetranuclear hydrolysis species $[Zr_4(OH)_8(OH_2)_{16}]^{8+}$ to a hexanuclear acetate species $Zr_6(O)_4(OH)_4(CH_3COO)_{12}$. The solution species $Zr_6(O)_4(OH)_4(CH_3COO)_{12}$ was preserved in crystals by slow evaporation of the aqueous solution. Single crystal diffraction reveals an uncharged hexanuclear cluster in solid $Zr_6(\mu_3\text{-}O)_4(\mu_3\text{-}OH)_4(CH_3COO)_{12}\cdot 8.5H_2O$. EXAFS measurements show that the structure of the hexanuclear zirconium acetate cluster in solution and solid state are identical.

Introduction

Zirconium shows at [Zr(IV)] > 10^{-4} M a strong tendency towards hydrolysis and polymerization [1], even at high $[H^+]$ concentration. There is a common agreement that the dominant hydrolysis species is the tetranuclear complex $[Zr_4(OH)_8(OH_2)_{16}]^{8+}$. The related crystal structure with the $[Zr_4(OH)_8(OH_2)_{16}]^{8+}$ unit was first analyzed by Clearfied and Vaughan [2] and has been since refined since then by several authors. The presence of the tetranuclear hydrolysis complex in aqueous solution was first independently described by Muha et al. [3] and Åberg [4] based on X-ray scattering measurements, and has been recently confirmed by Hagfeldt et al. [5] with Zr K-edge EXAFS spectroscopy.

The extraordinary stability of this tetranuclear complex makes it likely that acetate can replace only the terminal water molecules whereas the tetranuclear core is preserved [6].

There are only two studies which reported thermodynamic properties of zirconium hydroxo acetate complexes at low Zr concentration. Konunova et al. [7] investigated solutions at pH 2 – 4 with 0.005 – 0.02 M $ZrOCl_2$ and 0.01 – 0.02 M acetic acid by means of potentiometric titration. They suggested the formation of $[Zr(OH)_3CH_3COO]$ with a complexation constant of $\log \beta = 3.79 \pm 0.07$. Vladimirova et al. [8] repeated the study using a kinetic method with $6.18 \cdot 10^{-6}$ M $ZrOCl_2$ in the pH range of 0.82 – 1.64. A higher stability constant of $\log \beta^\circ = 6.18 \pm 0.05$ was found for the species $[Zr(OH)_2CH_3COO]^+$. Both studies suggested formation of monomeric Zr acetate complexes, although Konunova et al. did not exclude the additional formation of polymeric species. However, none of these two studies provided an independent spectroscopic validation of the assumed complex stoichiometry.

Several attempts were made to determine the structure of zirconium acetate species in solution and solid state. Ludwig and Schwartz [9] and Strauhan et al. [10] synthesized zirconium acetate in strictly water free solution and suggested, by using infrared (IR) spectroscopy, formation of the monomeric complex $Zr(CH_3COO)_4$ with bidentate coordinated acetate ligands. Paul et al. [11] isolated Zr(IV) oxo and hydroxo acetate complexes from reflux in pure acetic acid and suggested from IR spectroscopy a tetranuclear Zr complex with bidentate chelating and /or bidentate bridging coordination similar as earlier reported by Prozorovskaya [12]. Tosan et al. [6] suggested also tetranuclear species $[Zr_4(OH)_8(RCOO)_4]Cl_4$ (with R = H, CH_3) and suggested from IR spectra that the carboxylic groups bind in bidentate chelating coordination. Brenholm et al. [13] analyzed recently zirconium acetate solutions with small angle X-ray scattering and suggested that the zirconium species exists as extended oligomer chains of linked cyclic tetramers similar to the $[Zr_4(OH)_8(OH_2)_{16}]^{8+}$ complex. Solutions with zirconium carboxylates, mainly acetate, are widely used as precursor for synthesis of ZrO_2 nanoparticles and ZrO_2 ceramic material [14, 15]. There is a common agreement that the species in solution form the precursor in the subsequent sol/gel process and influence the structure and properties of the derived ceramics. Despite this technological importance, the complex structures of zirconium acetate species in solution and solid state are still not known which motivates a related study. The aim of our study is therefore to investigate the coordination and speciation of zirconium in aqueous acetic acid solution by Zr K-edge EXAFS spectroscopy, to preserve the limiting solution species by crystallization, and to determine the solid-state structure by single crystal diffraction.

Experimental section

Preparation of aqueous solutions. Two concentrated stock solutions were prepared (i) 1.0 M $ZrOCl_2 \cdot 8H_2O$ (Sigma Aldrich, p.a.), (ii) 2.0 M CH_3COOH (VWR, p.a.). A sample serie of 0.1 M Zr(IV) was prepared by addition of stock solution (i) to an appropriate amount of solution (ii) to obtain the following molar ratios of acetic acid / Zr(IV): 0, 0.1, 0.2, 0.3, 0.4. 0.5, 0.6, 0.8, 1.0, 1.5, 2.0, 3.5, 5.0, and 10.0. The pH value was adjusted to 1.5 with HCl and NaOH. In order to avoid kinetic effects [6] the aqueous samples were equilibrated for several weeks prior to EXAFS measurements.

Single crystal synthesis. Several attempts were made to obtain single crystals of Zr(IV) acetate from aqueous solution by variation of the synthesis conditions. The reported structure was obtained from a mixture of 5 mL 1.0 M $ZrOCl_2$ with 5 mL 1 M CH_3COOH. The initial pH of 0.30 was increased to 1.77 by adding 2 M ammonium acetate solution. The clear solution was slowly evaporated at room temperature. The Zr acetate crystals were then separated from co-precipitated crystals of the ligand.

EXAFS measurements. EXAFS measurements were performed in transmission mode using a Si(111) double-crystal monochromator on the Rossendorf Beamline [16] at the European Synchrotron Radiation Facility (Grenoble, France). Higher harmonics were rejected by two Rh coated mirrors. The Zr K-edge EXAFS spectra were collected at 25°C and ambient pressure by using ionization chambers filled with 25% argon and 75% nitrogen before the sample (I_0) and with pure argon after the sample (I_1) and the energy reference (I_2). For energy calibration, a Zr metal foil was measured simultaneously in transmission mode (first inflection point at 17998 eV). Data were collected in equidistant *k*-steps of 0.05 $Å^{-1}$ across the EXAFS region. The Zr K threshold energy for the EXAFS spectrum, $E_{k=0}$, was arbitrarily defined as E_0 = 18012 eV for all spectra. EXAFS data were extracted from the raw absorption spectra by standard methods including a spline approximation for the atomic background using the program WINXAS [17]. Data fitting was performed with EXAFSPAK [18]. Theoretical phase and amplitude functions were calculated with FEFF 9.4 [19] by using the crystal structures of $[Zr_4(OH)_8(H_2O)_{16}]Cl_6 \cdot 12H_2O$ [5] and $Zr_8O_4(OH)_4(CH_3COO)_{12} \cdot 8.5H_2O$ (this work). The FT peaks are shifted to lower values $R+\Delta$ relative to the true near-neighbour distances *R* due to the phase shift of the electron wave in the adjacent atomic potentials. This Δ shift is considered as

a variable during the shell fits. The amplitude reduction factor, S_0^2, was defined as 0.9 and fixed to that value in the data fits. The quantitative distribution of species in aqueous solutions was analyzed by Iterative Target Transformation Factor Analysis using the program ITFA from Rossberg et al. [20]. The standard deviations of relative concentrations were determined with the algorithm proposed by Malinowski [21].

X-ray diffraction. The single crystal X-ray data collection was carried out on a Bruker AXS SMART diffractometer at room temperature using Mo Kα radiation (λ=0.71073 Å) monochromatized by a graphite crystal. Data reduction was performed by using the Bruker AXS SAINT and SADABS packages. The structures were solved by direct methods and refined by full-matrix least squares calculation using SHELX [22, 23]. Anisotropic thermal parameters were employed for non-hydrogen atoms. The hydrogen atoms were treated isotropically with U_{iso} = 1.2 times the U_{eq} value of the parent atom. The hydrogen atoms were introduced in ideal positions. Crystal data and structure refinement details are summarized in Table 3. The crystallographic data for the structures have been deposited at the Cambridge Crystallographic Data Centre. The CCDC number is given in Table 3. Copies of the data can be obtained, free of charge, on application to CCDC, 12 Union Road, Cambridge CB2 1EZ, UK, fax: +44 1223 336033 or e-mail: deposit@ccdc.cam.ac.uk.

Results and discussion

First we identified the Zr(IV) hydrolysis species of the initial solution before the complexation with acetate. Figure 1 shows the Zr K-edge EXAFS spectrum and the corresponding Fourier transform of the aqueous sample with 0.1 M Zr(IV) at pH 1.5.

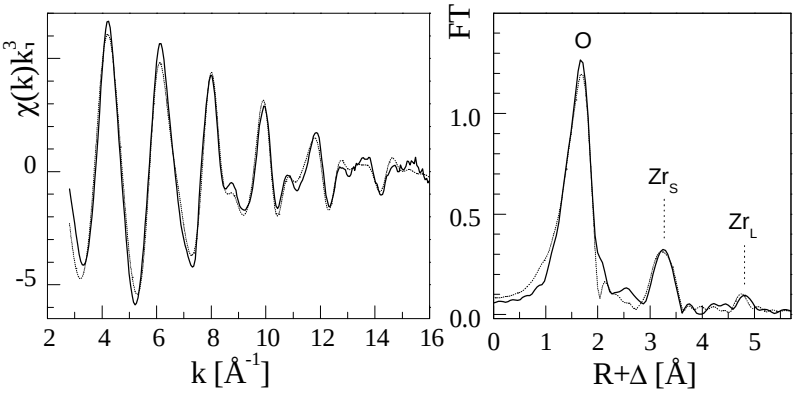

Figure 1. Zr K-edge k^3-weighted EXAFS data (left) and the corresponding Fourier transform (right) of an aqueous solution with 0.1 M $[Zr_4(OH)_8(H_2O)_{16}]Cl_6 \cdot 12H_2O$ at pH 1.5. This spectrum represents the initial Zr(IV) species $[Zr_4(OH)_8(OH_2)_{16}]^{8+}$. The spectrum reveals Zr backscattering peaks at short (Zr_S) and long (Zr_L) distance.

The Fourier transform reveals three peaks labelled with the symbol of the related backscattering atoms in the environment of the excited Zr atom. Table 1 summarizes the fit result.

Table 1. EXAFS fit parameters of the initial tetranuclear Zr(IV) complex of the aqueous solution with 0.1 M $[Zr_4(OH)_8(OH_2)_{16}]Cl_8 \cdot 12H_2O$ at pH 1.5.

Sample	Scattering path	R / Å	N	σ^2 / Å^2	$\Delta E_{k=0}$ /eV	F
Solid	Zr-O_1	2.169(2)	7.5(2)	0.0079(1)	-0.7	0.23
	Zr- Zr_S	3.620(3)	2.3(3)	0.0076(6)		
	Zr- Zr_L	5.14(1)	0.9(5)	0.005(2)		

R – interatomic distance, N – coordination number, σ^2 – Debye-Waller Factor, $\Delta E_{k=0}$ – threshold energy shift, F – error of data fit normalized to numbers of data points. Standard deviation of the last digit is given in parentheses. The error of distances is ± ~0.02 Å, the error of coordination numbers is ± ~20%.

The first peak reveals 8 direct coordinated oxygen atoms at an average Zr-O distance of 2.169(2) Å. It is followed by two peaks indicating a shorter Zr-Zr_S distance of 3.620(3) Å and a longer Zr-Zr_L distance of 5.14(1) Å. The shorter distance is related with two coordinated Zr atoms (fit error ± 20%), and the longer Zr distance with one Zr atom, characteristic for the tetranuclear hydrolysis complex $[Zr_4(OH)_8(H_2O)_{16}]^{8+}$, which has been described in detail before [4,5]. The experimental data range Δk = 3.0-16.0 Å^{-1} provides a spectral resolution of 0.12 Å. This is not sufficient to differentiate in the EXAFS fit between oxygen atoms from OH^- and H_2O because of their small distance differences, which are known from the crystal structure of $[Zr_4(OH)_8(H_2O)_{16}]Cl_6 \cdot 12H_2O$ [2, 5]. It should be mentioned that trimeric species, such as $Zr_3(OH)_4^{8+}$ and $Zr_3(OH)_9^{3+}$, which are suggested in the thermodynamic literature [24], are only of minor importance in the solution under discussion. These species would not contribute to the EXAFS scattering peak at 5.14(1) Å. The fact that the observed coordination number of this peak is close to one, as expected for the tetramer, indicates the predominant presence of $[Zr_4(OH)_8(OH_2)_{16}]^{8+}$.

The EXAFS spectra of the successive complex formation of 0.1 M Zr(IV) with CH_3COOH at pH 1.5 is shown in Figure 2. The spectrum of the initial solution without acetate is included. It is obvious that complexation occurs within the sample series. The carboxylic group deprotonates easily due to the strong Lewis acidity of Zr(IV), even at pH 1.5. That is over three orders of magnitude below the pK_a of acetic acid.

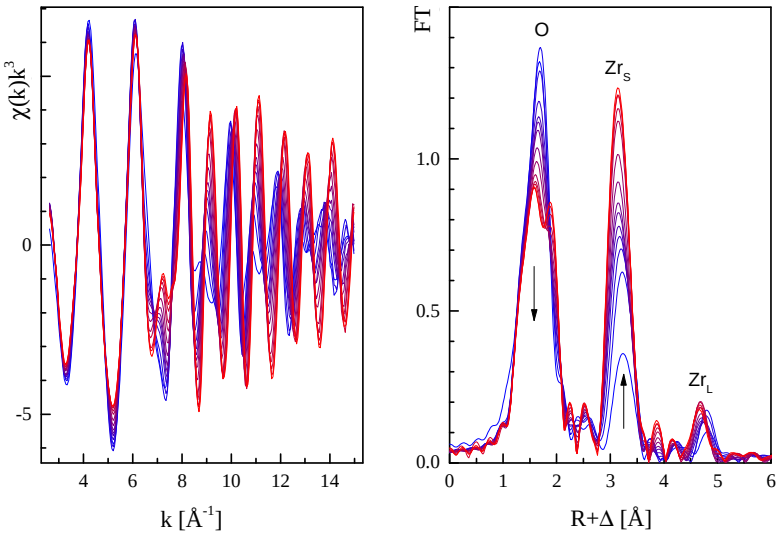

Figure 2. Zr K-edge k^3-weighted EXAFS data (left) and the corresponding Fourier magnitudes (right) of aqueous solution with 0.1 M Zr(IV), pH 1.5 and increasing concentration of CH_3COOH. Arrows indicate the trends in the spectral evolution. The intensity of the Zr backscattering peak at short distance (Zr_S) changes significantly whereas the intensity of Zr at long distance (Zr_L) remains largely unchanged.

Two arrows indicate the direction of the spectral evolution with increasing acetic acid concentration. The first peak, Zr-O, loses in intensity and undergoes a splitting. The second peak, Zr_S, increases in intensity compared with the initial species. The third peak, Zr_L, does not change significantly its intensity but shifts to shorter distances. The EXAFS spectra show several isosbestic points, suggesting equilibrium between two main solution species. The entire series of EXAFS spectra has been analyzed with factor analysis which reveals two dominating species. The quantitative fraction of the two species is shown in Figure 3 together with the extracted spectral components.

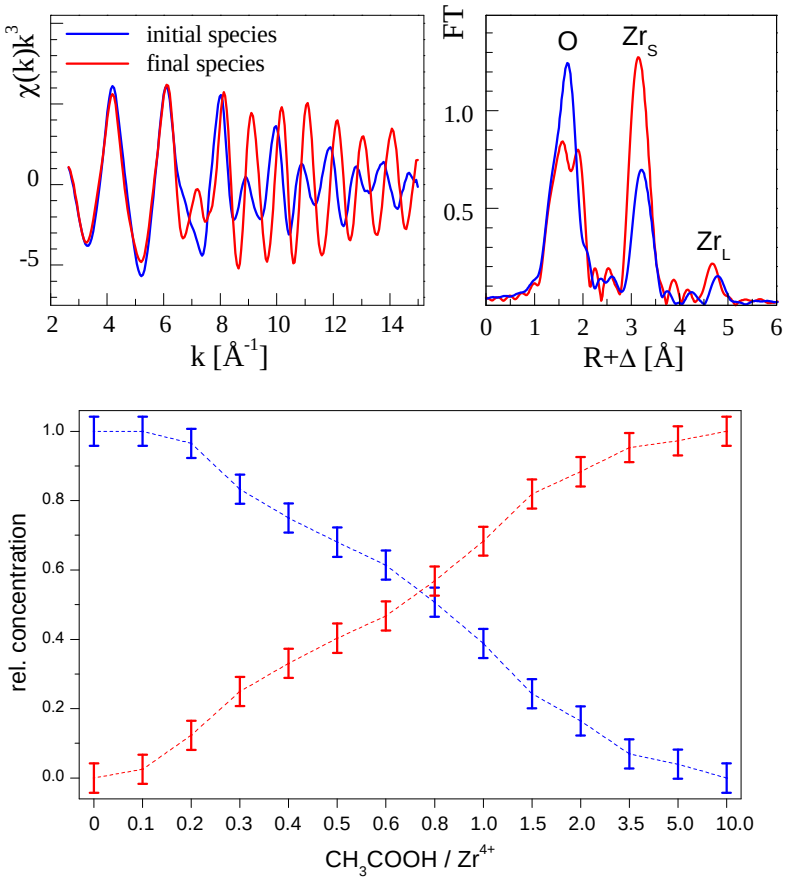

Figure 3. Factor analysis of EXAFS spectra. Top: EXAFS spectra (left) and corresponding Fourier transform magnitude (right) of the extracted two main components. Bottom: relative concentrations of the two components as function of the molar ligand / Zr^{4+} ratio. The blue colour represents the initial tetranuclear species $[Zr_4(OH)_8(H_2O)_{16}]^{8+}$, the red colour represents the hexanuclear complex $Zr_6(O)_4(OH)_4(CH_3COO)_{12}$.

The spectra of the initial and final species are similar but not completely identical with the first and last spectrum of the series. The small difference is a hint that the initial solution might not exclusively consist of $[Zr_4(OH)_8(H_2O)_{16}]^{8+}$, and furthermore, that there might exist an intermediate species of minor importance. It was not possible to extract these minor components as individual spectra. However, it is possible to extract important structural features of the main zirconium acetate species. It is obvious that the oxygen shell of the final species comprises different distances which result in the well pronounced splitting. The peak intensity of the Zr- Zr_S shell is just doubled compared to $[Zr_4(OH)_8(H_2O)_{16}]^{8+}$, which indicates that each of the excited Zr atoms has 4 Zr neighbors. The intensity of the Zr- Zr_L shell remains nearly unchanged compared to the initial species. This indicates the presence of one Zr atom at longer distance. Assuming that each Zr atom is symmetrically surrounded by

the same atomic arrangement, one can reasonably assume an octahedral arrangement of the Zr atoms. In such a hexanuclear polyhedron, each Zr atom has 4 nearer Zr_S neighbours and one Zr_L at a longer distance. An analysis of the related EXAFS fit is provided in Table 2.

Table 2. EXAFS fit parameters of the hexanuclear Zr(IV) acetate complex in solid state and aqueous solution of 0.1 M Zr(IV) in 1 M acetic acid at pH 1.5.

Sample	Scattering path	R / Å	N	σ^2 / Å^2	$\Delta E_{k=0}$ /eV	F
Solid	Zr-O_1	2.119(4)	4	0.0082(6)	0.9	0.23
	Zr-O_2	2.252(4)	4	0.0065(4)		
	Zr- Zr_S	3.545(2)	4	0.0055(1)		
	Zr- Zr_L	5.023(9)	1	0.0055(1)		
Solution	Zr-O_1	2.114(3)	4	0.0060(3)	- 0.1	0.33
	Zr-O_2	2.258(3)	4	0.0038(2)		
	Zr- Zr_S	3.524(2)	4	0.0046(1)		
	Zr- Zr_L	4.986(9)	1	0.0047(1)		

R – interatomic distance, N – coordination number, σ^2 – Debye-Waller Factor, $\Delta E_{k=0}$ – threshold energy shift, F – error of data fit normalized to numbers of data points. Coordination numbers are taken from the crystallographic data of the solid sample, $Zr_6(\mu_3\text{-}O)_4(\mu_3\text{-}OH)_4(CH_3COO)_{12}\cdot 8.5H_2O$ and fixed during the fit procedure. Standard deviation of the last digit is given in parentheses. The error of distances is ± ~0.02 Å.

Fitting of two distances, Zr-O_1 and Zr-O_2, to the first split peak is possible because the difference exceeds the resolution limit. The fit revealed the distances Zr-O_1 = 2.119(4) Å and Zr-O_2 = 2.252(4) Å. In the section describing the single crystal it will be shown that the short distance is related with μ_3-oxygen atoms and the long one with μ-O of carboxylate ligands. Various attempts have been made to preserve the limiting solution species of Zr acetate in a crystal in order to elucidate the full complex structure by single crystal diffraction. The success of this attempt can be verified by comparing the EXAFS spectrum of the limiting zirconium acetate solution species with the spectrum of the crystalline material. The comparison of the two spectra is shown in Figure 4. The EXAFS fit of solid sample is included in Table 2.

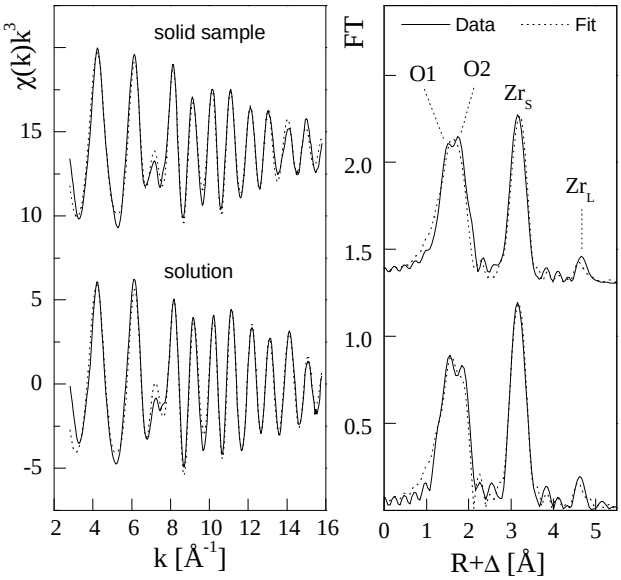

Figure 4. Zr K-edge k^3-weighted EXAFS data (left) and the corresponding Fourier transform (right) of the solid sample used for single crystal diffraction (top) and the aqueous solution of 0.1 M Zr(IV) in 1 M acetic acid at pH 1.5 (bottom).

It is evident that the main features in the spectra of the limiting solution species and that of the solid are identical. It can be expected that small differences in Zr-O distances result from influence of hydrogen bonds of water sphere on the solution species which differ from intramolecular arrangement of the complex in the crystal structure.

The molecular structure of the solid sample, which has been used for the EXAFS measurements, is determined by single-crystal diffraction analysis. Selected crystallographic data and structure refinement parameters are listed in Table 3. The molecular configuration is shown in Figure 5.

Table 3. Selected crystallographic data and structure refinement parameters of the solid sample $Zr_6(\mu_3\text{-}O)_4(\mu_3\text{-}OH)_4(CH_3COO)_{12}\cdot 8.5H_2O$.

Chemical formula	$C_{24}H_{36}O_{40.5}Zr_6$
F(000)	1488
Formula Mass	3039.70
Crystal system	Tetragonal
a/Å	12.605(2)
b/Å	12.605(2)
c/Å	13.626(3)
α/°	90.00
β/°	90.00
γ/°	90.00
Unit cell volume/Å^3	2165.0(7)
Temperature/K	296(2)
Space group	*I4/m*
No. of formula units per unit cell, *Z*	2
Radiation type	Mo-K_α
Absorption coefficient, μ/mm^{-1}	1.518
No. of reflections measured	1408
No. of independent reflections	1408
R_{int}	0.0000
Final R_1 values ($I > 2\sigma(I)$)	0.0677
Final $wR(F^2)$ values ($I > 2\sigma(I)$)	0.1783
Final R_1 values (all data)	0.0680
Final $wR(F^2)$ values (all data)	0.1784
Goodness of fit on F^2	1.080
CCDC number	1051013

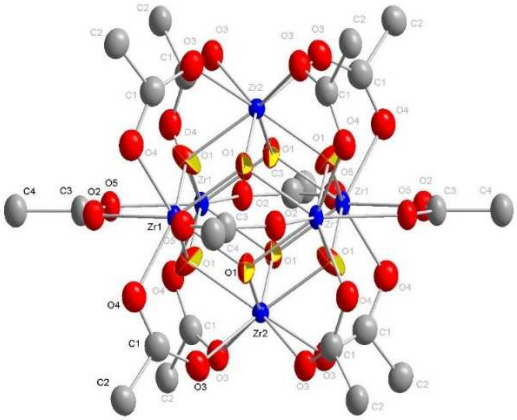

Figure 5. The hexameric Zr Cluster of the solid sample $Zr_6(\mu_3\text{-}O)_4(\mu_3\text{-}OH)_4(CH_3COO)_{12}\cdot 8.5H_2O$. Atomic positions are shown with 30% probability displacement ellipsoids. The atoms of the asymmetric unit are labeled in black, symmetry equivalent atoms depicted in grey. Hydrogen atoms are omitted for clarity.

The compound crystallizes in the tetragonal space group *I4/m* with 13 atoms in the asymmetric unit and two clusters in the unit cell. It forms a hexanuclear cluster with two symmetry independent zirconium atoms (Zr1, Zr2) and two symmetry independent acetic acid molecules with C1, C2, O3, O4 (Type 1) and C3, C4, O2, O5 (Type 2). The cluster forms a regular octahedron bridged by 8 μ_3-oxygen atoms (O1) and 12 bidentate *syn-syn* bridging acetate ligands (8 x Type 1, 4 x Type 2). Each Zr(IV) has a coordination number 8, caused by 4 μ_3-oxygen atoms O1 and 4 μ-O of carboxylate bridges. Hydrogen atoms have not been located during the structure refinement. The complex carries no excess charge as can be verified by the absence of charged counerions. The Zr-O distances of the carboxylate groups vary between 2.223(8) and 2.254(8) Å. The Zr-O1 bond shows a distance of 2.161(5) Å. The thermal ellipsoids of O1 and the charge balance in the structure suggest that O1 represents four μ_3-OH groups and four μ_3-O groups, which alternate across the faces of the octahedron. The fact that the oxygen atoms of chemically different oxo and hydroxo groups share the same crystallographic symmetry position seems to be a typical effect of this coordination geometry [25]. The packing of the clusters in the crystal structure is shown in Figure 6.

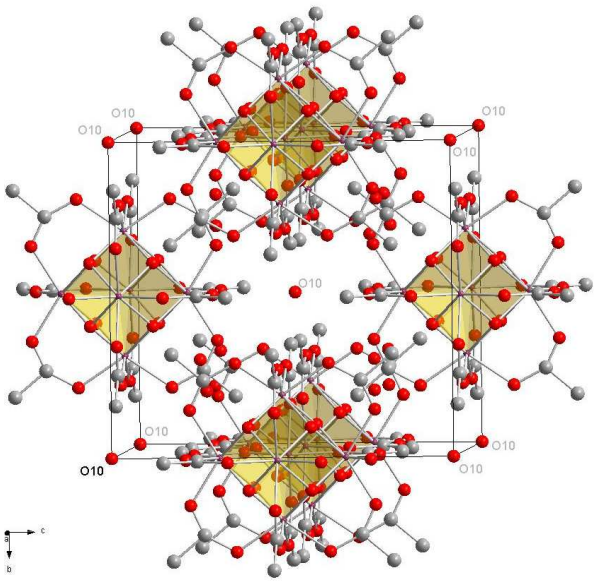

Figure 6. Arrangement of clusters in the unit cell of $Zr_6(\mu_3\text{-}O)_4(\mu_3\text{-}OH)_4(CH_3COO)_{12}\cdot 8.5H_2O$. *Hydrogen atoms are omitted for clarity.*

Non-bonded water molecules have been found in the space between the clusters. There are two types of water molecules with different arrangement to the cluster (see Figure S1, SI). The one with oxygen O6 is located on the general position with Wyckoff symmetry *16i*. It connects the

clusters via hydrogen bonds to the oxygen atom O4 of acetate molecule of type 1. Each of the 8 O4 atoms comprises two possible hydrogen bonds to O6 of the water molecules. The hydrogen bond weakens the Zr1-O4 bond which becomes slightly longer (2.254(8) Å) in comparison to the Zr2-O3 bond (2.236(7) Å). The clusters are linked to a three dimensional network though these hydrogen bonds. The acetate type 2 forms no hydrogen bonds. The second type water molecule with oxygen atom O10 is not involved in the hydrogen network but fills the voids between the clusters. The voids without O10 have a volume of 112.15 $Å^3$ and exploit 5.2% of the unit cell volume. O10 is located at a special position with Wyckoff symmetry *2a* and has an occupation factor of 0.5.

Several similar clusters of zirconium carboxylates with the general formula $Zr_6(O)_4(OH)_4(RCOO)_{12}$ were obtained from organic solutions, e.g. with R = But and $C(CH_3)_2Et$ [25], R = CH_3CH_2 [26], R = acrylate [27], $Zr6(O)_4(OH)_4(HGly)_4(Gly)_4$ [28] and $Zr_6(O)_4(OH)_4(OMc)_{12}$, Mc = methacrylate [29], and $Zr_6(\mu_3\text{-}OH)_5(OH)_4(\kappa^2\text{-bdmpza})_8$ with bdmpza = bis(3,5-dimethylpyrazol-1-yl)acetate [30]. A part of these clusters show carboxylate in bidentate chelating coordination whereas the investigated structure $Zr_6(\mu_3\text{-}O)_4(\mu_3\text{-}OH)_4(CH_3COO)_{12}\cdot 8.5H_2O$ shows exclusively bidentate bridging acetate ligands.

The zirconium atoms of these carboxylate stabilized hexanuclear clusters show usually a coordination number of 8. It should be noted that tetravalent actinide elements (An) form similar hexanuclear clusters with acetate and other carboxylates [31-40]. They show, related with their larger ionic radii [42], usually a coordination number of 9. Figure 7 shows the trend of the average metal-metal distances in the hexanuclear clusters of $^{[8]}Zr^{4+}$ and the $^{[9]}An^{4+}$ elements Th(IV), U(IV), Np(IV) and Pu(IV) in relation to the metal ion radii r_i.

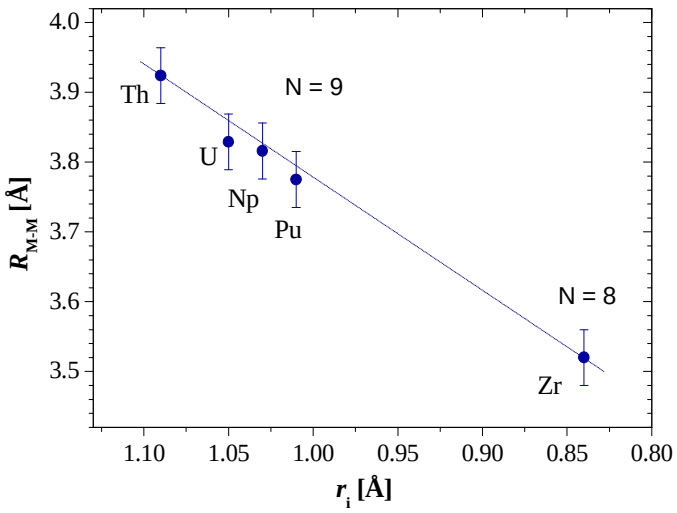

Figure 7. Metal-metal distances R_{M-M} and related coordination numbers N in hexanuclear $M_6(O)_4(OH)_4(RCOO)_{12}$ clusters as function of the metal radii r_i.

The increased coordination number of the *5f* elements possess in addition to the 4 μ_3-O from oxo and hydroxo groups and 4 oxygen atoms from carboxylates one single terminal solvent molecule. This correlation reveals a relationship of metal radius and cluster size and demonstrates large flexibility of this specific coordination mode.

The similarity of the EXAFS spectra of the Zr acetate species in aqueous solution and the crystalline sample, as shown in Figure 4, suggest that the limiting species is a charge neutral complex with the stoichiometry $Zr_6(\mu_3\text{-}O)_4(\mu_3\text{-}OH)_4(RCOO)_{12}$. With this knowledge and the known structure of the initial solution species $[Zr_4(OH)_8(OH_2)_{16}]^{8+}$ we can formulate the reaction scheme as follows:

$$3\ Zr_4(\mu_2\text{-}OH)_8(H_2O)_{16}^{8+} + 24\ CH_3COOH \rightarrow 2\ Zr_6(\mu_3\text{-}O)_4(\mu_3\text{-}OH)_4(CH_3COO)_{12} + 56\ H_2O + 24\ H^+$$

The formation of the hexanuclear complex $Zr_6(O)_4(OH)_4(CH_3COO)_{12}$ requires the destruction of the initial tetranuclear complex and the formation an intermediate species. ^1H and ^{13}C NMR spectra provides hints to the existence of such intermediate species (see supporting information, Figures S2-S4). The suggestion that zirconium acetate forms tetranuclear species with bidentate chelating acetate ligands [6,11,12] could not be confirmed. Due to the high stability it might be assumed that $Zr_4(OH)_8(H_2O)_{16}^{8+}$ polymerizes further by linking two tetranuclear complexes to an octanuclear one. Octanuclear Zr(IV) hydrolysis species were experimentally observed by [43]. The authors identified with small-angle X-ray scattering a hydrolysis complex $Zr_8(OH)_{20}(H_2O)_{24}^{12+}$. We can exclude the formation of significant amounts of an octanuclear complex in presence of acetate. Such complex could be identified with EXAFS spectroscopy by a next-neighbour sequence of $Zr_S = 3$, $Zr_{L1} = 3$, and $Zr_{L2} = 1$.

Conclusions

This study was performed to determine the structure of Zr acetate species in solution under equilibrium conditions. The presence of a hexanuclear Zr(IV) acetate complex in aqueous solutions of 0.1 M Zr(IV) at pH 1.5 was identified by means of Zr K-edge EXAFS

measurements. This solution species was preserved in crystals of $Zr_6(\mu_3\text{-}O)_4(\mu_3\text{-}OH)_4(CH_3COO)_{12}\cdot 8.5H_2O$. The comparison of the complex in solution and solid state allows the identification of the hexanuclear species $Zr_6(\mu_3\text{-}O)_4(\mu_3\text{-}OH)_4(CH_3COO)_{12}$ as dominant species in solution. The hexanuclear acetate species $Zr_6(O)_4(OH)_4(CH_3COO)_{12}$ cannot be formed directly from initial tetranuclear hydrolysis species $[Zr_4(OH)_8(OH_2)_{16}]^{8+}$. It is likely that the tetranuclear species will be transferred in a first step in an intermediate mononuclear or binuclear species which may act as building block of the thermodynamically favourable hexanuclear species.

ASSOCIATED CONTENT

The Supporting information is available free of charge on the ACS Publication website at DOI: (has to be filled by publisher)

Crystallographic data of $Zr_6(\mu_3\text{-}O)_4(\mu_3\text{-}OH)_4(CH_3COO)_{12}\cdot 8.5H_2O$ (CIF), H,C-HMBC and H,H-EXSY NMR spectra of Zr-acetate solution complex.

AUTHOR INFORMATION

Corresponding author

Christoph Hennig, E-mail: hennig@esrf.fr

Notes

The authors declare no competing financial interest

REFERENCES

[1] (a) Zielen, A.J.; Connick, R.E. J. *Am. Chem. Soc.* **1956**, 78, 5785; (b) Walther, C., Rothe, J., Fuss, M., Büchner, S., Koltov, S., Bergmann, T. *Anal. Bioanal. Chem.* **2007**, *388*, 409.

[2] Clearfield, A.; Vaughan, P.A. *Acta Cryst.* **1956**, 9, 555.

[3] Muha, G. M.; Vaughan, P. A. *J. Chem. Phys.* **1960**, 33, 194.

[4] Åberg, M. Acta. *Chem. Scand.* **1977**, A 31 (3) , 171.

[5] Hagfeldt, C.; Kessler, V.; Persson, I. *Dalton Trans.* **200**4, 2142.

[6] Tosan, J. L.; Durand, B.; Roubin, M.; Chassagneux, F. B.; Bertin, F. *J. Non-Cryst. Solids* **1994**, 168, 23.

[7] Konunova, T.B.; Popov, M.S.; Kuang, C. *Russian J. Inorg. Chem.* **1969**, 14 (8), 1084.

[8] Vladimirova, Z. A.; Prozorovskaya, N. Z.; Komissarova, L. N. *Russian J. Inorg. Chem.* **1973**, 18 (3), 368.

[9] Ludwig, J.; Schwartz, D. *Inorg. Chem.* **1970**, 9, 607.

[10] Straughan, B.P.; Moore, W.; McLaughlin, R. *Spectrochim. Acta* **1986**, 42A (4), 451.

[11] Paul, R. C.; Baidya, O. B.; Kumar, R. C. *Aust. J. Chem.* **1976**, 29, 1605.

[12] Prozorovskaya, Z. N.; Petrov, K. I.; Komissarova, L. N. *Russian J. Inorg. Chem.* **1968**, 13 (4), 505.

[13] Bremholm, M.; Birkedal H.; Brummerstedt Iversen B.; Pedersen J.S.
J. Phys. Chem. C **2015**, 119 (22), 12660.

[14] Geiculescu, A.C.; Spencer, H.G. *J. Sol-Gel Sci. Technol.* **2000**, 17, 25.

[15] De Keukeleere, K.; De Roo, J.; Lommens, P.; Martins, J.C.; Van Der Voort, P.; Van Driessche, I. *Inorg. Chem.* **2015**, *54* (7), 3469.

[16] Matz, W.; Schell, N.; Bernhard, G.; Prokert, F.; Reich, T.; Clauβner, J.; Oehme, W.; Schlenk, R.; Dienel, S.; Funke, H.; Eichhorn, F.; Betzl, M.; Pröhl, D.; Strauch, U.; Hüttig, G.; Krug, H.; Neumann, W.; Brendler, V.; Reichel, P.; Denecke, M.A.; Nitsche, H. *J. Synchrotron Rad.*, **1999**, 6, 1076.

[17] Ressler, T. *J. Synchr. Rad.* **1998**, 5, 118.

[18] George, G.N.; Pickering, I.J. *EXAFSPAK, a suite of computer programs for analysis of X-ray absorption spectra*, Stanford Synchrotron Radiation Laboratory, Stanford, **2000**.

[19] Rehr, J.J.; Kas, J.J.; Vila, F.D.; Prange, M.P.; Jorissen, K. *Phys. Chem. Chem. Phys.*, **2010**, 12, 5503.

[20] Rossberg, A.; Reich, T.; Bernhard, G. *Anal. Bioanal. Chem.* **2003**, *376*, 631.

[21] Malinowski, E. R. *Anal. Chim. Acta* **1980**, *122*, 327.

[22] Sheldrick, G.M. SHELXS-97, Program for the Solution of Crystal Structures, Universität Göttingen, **1997**.

[23] Sheldrick, G.M. SHELXL-97, Program for the Crystal Structure Refinement, Universität Göttingen, **1997**.

[24] Brown, P.L.; Curti, E.; Grambow, B.; Ekberg, C.; Mompean, F.J.; Perrone, J., Illemassène, M. *Chemical Thermodynamics Vol. 8: Chemical Thermodynamics of Zirconium* (OECD, NEA-TDB) Elsevier, Amsterdam, **2005**.

[25] Piszczek, P.; Radtke, A.; Grodzicki, A.; Wojtczak, A.; Chojnacki, J. *Polyhedron* **2007**, 26, 679.

[26] Mos, R.B.; Nasui, M.; Petrisor, T.; Gabor, M.S.; Varga, R.A.; Ciontea, L. J. *Anal. Appl. Pyrol.* **2012**, 97, 137.

[27] Puchberger, M.; Kogler; F.R.; Jupa, M.; Gross, S.; Fric, H.; Kickelbick, G.; Schubert, U. *Eur. J. Inorg. Chem.* **2006**, 3283.

[28] Pappas, I.; Fitzgerald, M.; Huang, X.-Y.; Li, J.; Pan, L. *Cryst. Growth Des.* **2009**, 9 (12), 5213.

[29] Kickelbick, G.; Schubert, U. *Chem. Ber./Recueil* **1997**, 130, 473.

[30] Otero, A.; Fernández-Baeza, J.; Antinolo, A.; Tejeda, J.; Lara-Sánchez, A.; Sánchez-Barba, L.; Fernández-López, M.; López-Solera, I. *Inorg. Chem.* **2004**, 43, 1350.

[31] Takao, S.; Takao, K.; Kraus, W.; Emmerling, F.; Scheinost, A.C.; Bernhard, G.; Hennig, C. *Eur. J. Inorg. Chem.* **2009**, 4771.

[32] Takao, K.; Takao, S.; Scheinost, A.C.; Bernhard, G.; Hennig, C. *Inorg. Chem.*, **2012**, 51, 1336.

[33] Berthet, J.C.; Thuéry, P.; Ephritikhine, M. *Chem. Commun.*, **2005**, 3415.

[34] Nocton, G.; Burdet, F.; Pécaut, J.; Mazzanti, M. *Angew. Chem. Int. Ed.*, **2007**, 46, 7574.

[35] Nocton, G.; Pécaut, J; Filinchuk, Y.; Mazzanti, M. *Chem. Commun,*. **2010**, 46, 2757.

[36] Mougel, V.; Biswas, B.; Pécaut, J.; Mazzanti, M. *Chem. Commun,*. **2010**, 46, 8648.

[37] Biswas, B.; Mougel, V.; Pecaut, J.; Mazzanti, M. *Angew. Chem. Int. Ed.*, **2011**, 123, 5863.

[38] Diwu, J.; Wang, S.; Albrecht-Schmitt, E. *Inorg. Chem.*, **2012**, 51, 4088.

[39] Hennig, C.; Takao, S.; Takao, K.; Weiss, S.; Kraus, W.; Emmerling, F.; Scheinost, A.C. *Dalton Trans.* **2012**, 41, 12818.

[40] Knope, K.; Soderholm, L. *Inorg. Chem.* **2013**, 52, 6770.

[41] Zhang, Y.; Karatchevtseva, I.; Kadi, F.; Lu, K.; Yoon, B.;Price, J.R. *Polyhedron* **2015**, 87, 377.

[42] Shannon, R.D. *Acta Cryst.* **1976**, A32, 751.

[43] Singhal, A.; Toth, L.M. *J. Am. Chem. Soc.* **1996**, 118, 11529.

Graphical Abstract